1. Optimal λ for SL-ALSH

In this section, we show that $\rho^{(l_2)}$ is minimized when $\lambda = \sqrt{d}/\left\|w\right\|_2$.

Let the weight vector w' be $w' = \lambda w$, where $\lambda > 0$. For any o and q, since $d_{w'}(o,q) = \lambda d_w(o,q)$, the problem of (R_1, R_2)-NNS for w is equivalent to the problem of $(\lambda R_1, \lambda R_2)$-NNS for w'. Hence, for SL-ALSH, the minimum value of $\rho^{(l_2)}$ is computed as follows:

$$\rho^{(l_2)}_{min} = \min_{\lambda,r,U} \frac{\ln(p^{(l_2)}(\sqrt{\sum_i (1-\lambda w_i)^2 + \lambda R_1 - \frac{\lambda}{12} w^- U^4}))}{\ln(p^{(l_2)}(\sqrt{\sum_i (1-\lambda w_i)^2 + \lambda R_2 - \frac{\lambda}{12}(1+w^-) U^4}))}, \quad (1)$$

where

$$\begin{aligned} p^{(l_2)}(\delta) &= Pr_{h_{l_2}\in\mathcal{H}}[h_{l_2}(o) = h_{l_2}(q)] \\ &= 1 - 2\Phi(-r/\delta) - \frac{2}{\sqrt{2\pi}(r/\delta)}(1 - e^{-(r/\delta)^2/2}) \end{aligned} \quad (2)$$

and $\Phi(x) = \int_{-\infty}^{x} \frac{1}{\sqrt{2\pi}} e^{-x^2/2}\,dx$.

Let $p_r(x) = p^{(l_2)}(\sqrt{x})$. From Equation 2, we observe that, for any $\alpha > 0$,

$$p_r(x) = p_{\alpha r}(\alpha^2 x). \quad (3)$$

Let $\kappa_1(\lambda, U) = \sum_i (1-\lambda w_i)^2 + \lambda R_1 - \frac{\lambda}{12} w^- U^4$ and $\kappa_2(\lambda, U) = \sum_i (1-\lambda w_i)^2 + \lambda R_2 - \frac{\lambda}{12}(1+w^-)U^4$. We then consider the minimum value of following function

$$\rho^{(l_2/\lambda)}(r, U, \lambda) = \frac{\ln(p_r(\kappa_1(\lambda,U)/\lambda))}{\ln(p_r(\kappa_2(\lambda,U)/\lambda))}. \quad (4)$$

Lemma 1. *For $r > 0$, $0 < U \le \pi$, and $\lambda > 0$,*

$$\rho^{(l_2/\lambda)}_{min} = \min_{r,U,\lambda} \rho^{(l_2/2)}(r,U,\lambda) = \rho^{(l_2)}_{min}. \quad (5)$$

Proof. Let r^*, U^*, and λ^* be the optimal r, U, and λ that minimize $\rho^{(l_2)}$, i.e., for $r > 0$, $0 < U \le \pi$, and $\lambda > 0$,

$$\rho^{(l_2)}_{min} = \frac{\ln(p_{r^*}(\kappa_1(\lambda^*, U^*)))}{\ln(p_{r^*}(\kappa_2(\lambda^*, U^*)))} \le \frac{\ln(p_r(\kappa_1(\lambda, U)))}{\ln(p_r(\kappa_2(\lambda, U)))} \quad (6)$$

Based on Equations 3 and 6, we have

$$\begin{aligned} \frac{\ln(p_r(\kappa_1(\lambda,U)/\lambda))}{\ln(p_r(\kappa_2(\lambda,U)/\lambda))} &= \frac{\ln(p_{r\sqrt{\lambda}}(\kappa_1(\lambda,U)))}{\ln(p_{r\sqrt{\lambda}}(\kappa_2(\lambda,U)))} \\ &\ge \frac{\ln(p_{r^*}(\kappa_1(\lambda^*,U^*)))}{\ln(p_{r^*}(\kappa_2(\lambda^*,U^*)))} \\ &= \rho^{(l_2)}_{min}, \end{aligned}$$

and the equality holds when $r = r^*/\sqrt{\lambda^*}$, $\lambda = \lambda^*$, and $U = U^*$. □

According to Lemma 1

$$\rho^{(l_2)}_{min} = \min_{\lambda,r,U} \frac{\ln(p^{(l_2)}(\sqrt{\frac{\sum_i (1-\lambda w_i)^2}{\lambda} + R_1 - \frac{1}{12} w^- U^4}))}{\ln(p^{(l_2)}(\sqrt{\frac{\sum_i (1-\lambda w_i)^2}{\lambda} + R_2 - \frac{1}{12}(1+w^-) U^4}))}. \quad (7)$$

We have Lemma 2 as follows:

Lemma 2. *$p_r(x)$ is strictly convex w.r.t x, where $x > 0$.*

Proof. We first consider a special case $r = 1$. Let $p_1(x) = p_r(x)|_{r=1}$. The second derivative of $p_1(x)$ w.r.t x can be computed as follows:

$$\frac{\partial^2 p_1(x)}{\partial x^2} = \frac{\sqrt{2}}{4\sqrt{\pi}}(x^{-2.5} e^{-\frac{1}{2x}} + x^{-1.5}(1 - e^{-\frac{1}{2x}})).$$

It can be verified that $\frac{\partial^2 p_1(x)}{\partial x^2} > 0, \forall x > 0$, which means $p_1(x)$ is strictly convex for x, where $x > 0$.

Next, we show the convexity of $p_r(x)$ holds for all $r > 0$. For any $0 < \alpha < 1, x_1 > 0, x_2 > 0, r > 0$, based on Equation 3, we derive that

$$\begin{aligned} &\alpha p_r(x_1) + (1-\alpha) p_r(x_2) \\ &= \alpha p_1(x_1/r^2) + (1-\alpha) p_1(x_2/r^2) \\ &< p_1(\alpha x_1/r^2 + (1-\alpha) x_2/r^2) \\ &= p_r(\alpha x_1 + (1-\alpha) x_2). \end{aligned}$$

Thus, according to the definition of convex function (Bertsekas et al., 2003), $p_r(x)$ is a strictly convex function w.r.t x, where $x > 0$. □

Let $f(x) = \ln(p_r(x)) = \ln(p^{(l_2)}(\sqrt{x}))$. Since $p_r(x) > 0, \forall x > 0$, $f(x)$ is logarithmically convex. Thus, we have

$$f''(x) f(x) > (f'(x))^2. \quad (8)$$

Let $g(x) = f'(x)/f(x)$. We get Lemma 3 as follows:

Lemma 3. *$g(x)$ is monotonically increasing w.r.t x, where $x > 0$.*

Proof. From Equation 8, it is easy to see that

$$g'(x) = \frac{f(x) f''(x) - f'(x)^2}{f(x)^2} > 0.$$

Thus, Lemma 3 is proved. □

According to Lemma 3, $g(x) < g(x + c), \forall c > 0$, i.e.,

$$f'(x)/f(x) > f'(x+c)/f(x+c). \quad (9)$$

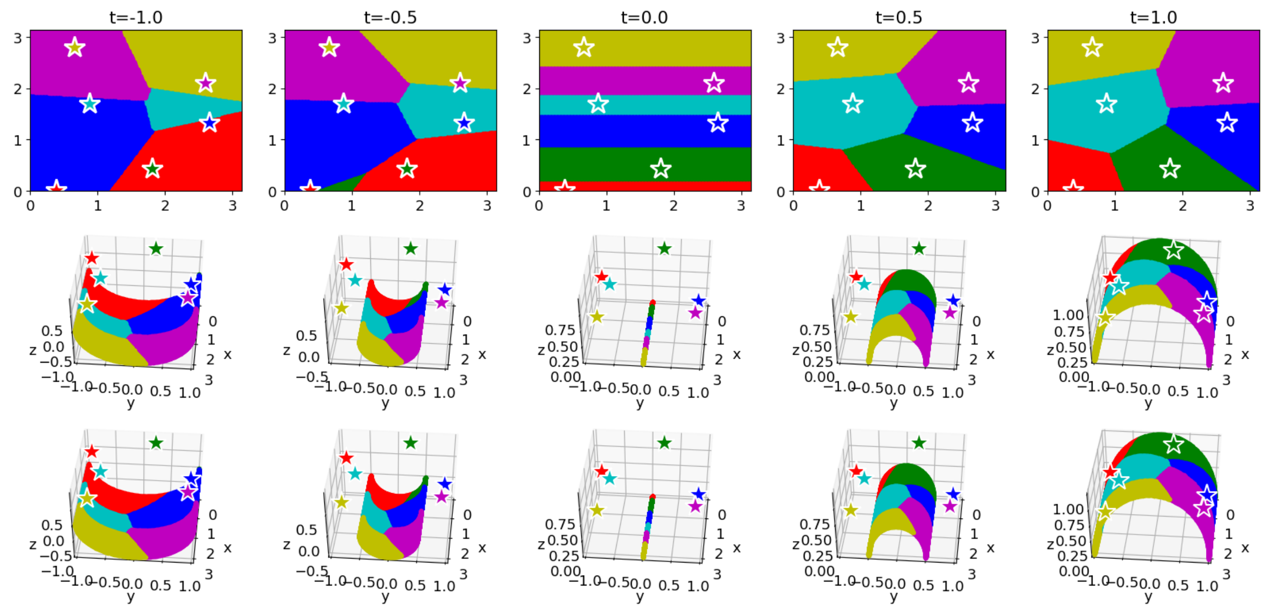

Figure 1. Spherical asymmetric transformation visualization on the 2-dimensional synthetic data objects.

We define $\rho(x)$ as follows:

$$\rho(x) = \frac{\ln(p^{(l_2)}(\sqrt{x}))}{\ln(p^{(l_2)}(\sqrt{x+c}))} = \frac{f(x)}{f(x+c)}. \quad (10)$$

Then, we achieve Lemma 4 as follows:

Lemma 4. *$\rho(x)$ is monotonically increasing w.r.t x, where $x > 0$.*

Proof. The derivative of $\rho(x)$ w.r.t x is computed as:

$$\rho'(x) = \frac{f'(x)f(x+c) - f(x)f'(x+c)}{f(x+c)^2}.$$

From Equation 9, $f'(x)f(x+c) - f(x)f'(x+c) > 0$ given the fact $f(x) < 0, \forall x > 0$. Thus, $\rho'(x) > 0, \forall x > 0$. Lemma 4 is proved. □

Theorem 5. *$\rho_{min}^{(l_2)}$ is achieved when $\lambda = \sqrt{d}/\left\|w\right\|_2$.*

Proof. Based on the condition $p_1 > p_2$, we have

$$R_2 - R_1 > \frac{1}{12}U^4.$$

Let $x = \frac{\sum_i (1-\lambda w_i)^2}{\lambda} + R_1 - \frac{1}{12}w^- U^4$ and $c = R_2 - R_1 - \frac{1}{12}U^4 > 0$. Then, $\rho(x)$ as defined by Equation 10 has the same formula with the function we want to minimize in Equation 7 and has the minimum value when $\frac{\sum_i (1-\lambda w_i)^2}{\lambda}$ is minimized because of Lemma 4. According to the AM-GM inequality, $\frac{\sum_i (1-\lambda w_i)^2}{\lambda}$ is minimized when $\lambda = \sqrt{d}/\left\|w\right\|_2$. Therefore, $\rho_{min}^{(l_2)}$ is achieved when $\lambda = \sqrt{d}/\left\|w\right\|_2$. □

By replacing $\lambda = \sqrt{d}/\left\|w\right\|_2$ and $\eta = \sqrt{d}\left\|w\right\|_2$ into Equation 7, we have

$$\rho_{min}^{(l_2)} = \min_{r,U} \frac{\ln(p^{(l_2)}(\sqrt{2\eta - 2(1+2w^-) + R_1 - \frac{1}{12}w^- U^4}))}{\ln(p^{(l_2)}(\sqrt{2\eta - 2(1+2w^-) + R_2 - \frac{1}{12}(1+w^-)U^4}))}.$$

2. Transformation Visualization

In order to show how the spherical asymmetric transformation works, we visualize the spherical asymmetric transformation on synthetic 2-dimensional data objects in Figure 1. The synthetic 2-dimensional data objects are generated uniformly at random from $[0, \pi]^2$. We randomly sample 6 data objects and mark all of them as stars with various colors. Then, we generate 40,000 queries with equal distance on each dimension from $[0, \pi]$. We plot each query with the same color of its NN over d_w. The results of the data objects and queries in the original Euclidean space $\mathbb{R}^2$ are shown in the first row of Figure 1.

Next, we visualize the data objects and queries in the transformed space. According to the vector transformations P and Q as defined by Equations 9 and 10 in the paper, each object and query will be mapped to a 2-dimensional manifold in a 4-dimensional space, i.e., a data object $o = [o_1, o_2]$ is mapped to

$$P(o) = [\cos(o_1), \cos(o_2), \sin(o_1), \sin(o_2)], \quad (11)$$

and a query $q = [q_1, q_2]$ is mapped to

$$Q(q, w) = [w_1 \cos(q_1), w_2 \cos(q_2), w_1 \sin(q_1), w_2 \sin(q_2)]. \quad (12)$$

For a weight vector w, since the L_1 norm of w does not change the order of NNS results over d_w, a d-dimensional weight vector w indeed has only $(d-1)$ degree of freedom, For example, let $w = (w_1, w_2)$ and $w_2 > 0$. A query q with w has as same order of NNS results as q with $w' = (w_1/w_2, 1)$. Notice that 4-dimensional objects are hard to visualize. In order to straightforwardly visualize the data objects and queries in the transformed space, we set the weight vector as $w = (t, 1)$ and consider five cases of t for visualization, where $t \in \{-1.0, -0.5, 0.0, 0.5, 1.0\}$. From Equation 12, $Q(q, w) = [t \cos(q_1), \cos(q_2), t \sin(q_1), \sin(q_2)]$. We observe that the second and fourth dimensions of $Q(q, w)$ are independent of w and have only 1 degree of freedom. Thus, we visualize the data objects and queries in the transformed space with $P'(o) = [o_2, \cos(o_1), \sin(o_1)]$ and $Q'(q, w) = [q_2, t \cos(q_1), t \sin(q_1)]$, respectively. The data objects are of the same color with their corresponding objects in the original space. For the queries, we plot each query with the same color of its NN over L_2 distance and Angular distance in the transformed space. The results are shown in the second and third row of Figure 1.

From Figure 1, we observe that the figures of these two rows are nearly identical. A clear one-to-one correspondence for the data objects and queries between original space and transformed space can be easily found. These results empirically support that our proposed spherical asymmetric transformation can indeed preserve the NNs of queries. Note that the spherical asymmetric transformation is essentially dimension-wise. Therefore, the intuition from visualizing low-dimensional space can be applied to high-dimensional space as well.

References

Bertsekas, D. P., Nedi, A., Ozdaglar, A. E., et al. Convex analysis and optimization. 2003.